

# Optimal Operation of Flexible Distribution Networks for Security Improvement Considering Active Management

**Liu, Jia; Zeng, Pingliang; Xing, Hao; Li, Yalou; Wu, Qiuwei**

*Published in:*
CSEE Journal of Power and Energy Systems

*Link to article, DOI:*
10.17775/CSEEJPES.2020.02860

*Publication date:*
2023

*Document Version*
Publisher's PDF, also known as Version of record

# Optimal Operation of Flexible Distribution Networks for Security Improvement Considering Active Management

Jia Liu, *Member*, *IEEE*, Pingliang Zeng, *Senior Member*, *IEEE*, Hao Xing, *Member*, *IEEE*, Yalou Li, *Member*, *IEEE*, and Qiuwei Wu, *Senior Member*, *IEEE*

***Abstract*—This paper presents a stochastic optimal operation problem of gas turbine integrated distribution networks in the presence of active management schemes, which is formulated as a multi-objective chance-constrained mixed integer nonlinear programming problem. The control variables are the on-load tap-changer tap position, the power provided by the distributed generation (DG), the DG power factor angle, the load participating in demand side management and the switch status. The objectives defined in this paper are to simultaneously minimize the expectation cost and variation coefficient of security distance. Uncertainties related to DG output and load fluctuation and fault power restoration under contingencies are also considered in the optimization problem. The collaboration of normal boundary intersection and the dynamic niche differential evolution algorithm is proposed to handle the optimal operation mode. Simulation results are presented and demonstrate the effectiveness of the proposed model. Compared with the operation result without the consideration of security, the security-constrained operation can reduce the expectation cost. Therefore, the proposed optimization is reasonable and valuable.**

***Index Terms*—Active management, flexible distribution networks, optimal operation, security improvement, uncertainties.**

## NOMENCLATURE

### A. Sets and vectors

| | |
|---|---|
| $\Phi^{(b)}(\Phi^{(j)})$ | Set of buses (connected to bus $j$). |
| $\Phi^{(d)}$ | Set of DG buses. |
| $\Phi^{(r)}$ | Set of substation buses. |
| $\Phi^{(f)}$ | Set of feeder sections. |
| $\Phi^{(k)}$ | Set of hyperplanes. |
| $\Phi^{(l)}(\Phi^{(lt)})$ | Set of branches (with transformers). |
| $\Phi^{(s)}$ | Set of switches. |
| $\Phi^{(sc)}$ | Set of scenarios. |
| $\Phi^{(t)}$ | Set of periods. |
| $W_f(W_{f0})$ | Vector of operating point (on security region boundary $B_k$). |

### B. Variables

| | |
|---|---|
| $\mathrm{SD}_k$ | Security distance of $F_k$ (MVA). |
| $U_i$ | Voltage magnitude at bus $i$ (p.u.). |
| $V_i$ | Square of voltage magnitude at bus $i$ (p.u.$^2$). |
| $I_{ij}$ | Current magnitude at branch $ij$ (kA). |
| $L_{ij}$ | Square of current magnitude at branch $ij$ (kA$^2$). |
| $C^{\mathrm{S}}_{\mathrm{sc,t}}$ | Switching cost in scenario $sc$ and time period $t$ ($\times 10^4$ \$). |
| $C^{\mathrm{OM}}_{\mathrm{sc,t}}$ | DG operation cost in scenario $sc$ and time period $t$ ($\times 10^4$ \$). |
| $C^{\mathrm{AM}}_{\mathrm{sc,t}}$ | DG AM cost in scenario $sc$ and time period $t$ ($\times 10^4$ \$). |
| $C^{\mathrm{P}}_{\mathrm{sc,t}}$ | Cost of energy injected from the upstream grid in scenario $sc$ and time period $t$ ($\times 10^4$ \$). |
| $C^{\mathrm{LOSS}}_{\mathrm{sc,t}}$ | Loss cost in scenario $sc$ and time period $t$ ($\times 10^4$ \$). |
| $C^{\mathrm{DSM}}_{\mathrm{sc,t}}$ | DSM cost in scenario $sc$ and time period $t$ ($\times 10^4$ \$). |
| $\mathrm{EVSD}_{\mathrm{sc}}$ | SD Expectation value in scenario $sc$ (MVA). |
| $\mathrm{SDSD}_{\mathrm{sc}}$ | Standard deviation of SD in scenario $sc$ (MVA). |
| $P^{\mathrm{loss}}_{\mathrm{sc,t}}$ | Total power loss in scenario $sc$ and period $t$ (MW). |
| $P^{\mathrm{sub}}_{\mathrm{sc,t}}$ | Power purchased from the upper grid in scenario $sc$ and period $t$ (MW). |
| $P^{\mathrm{L,DSM}}_{\mathrm{i,sc,t}}$, $Q^{\mathrm{L,DSM}}_{i}$ | Active (MW) and reactive (Mvar) loads that participate in DSM at bus $i$ in scenario $sc$ and period $t$. |
| $P^{\mathrm{WTG}}_{\mathrm{i,sc,t}}$, $P^{\mathrm{PVG}}_{\mathrm{i,sc,t}}$ | Output powers of WTGs and PVGs at bus $i$ in scenario $sc$ and period $t$ (MW). |
| $P_j, Q_j$ | Total active (MW) and reactive (Mvar) power injections at bus $j$. |

Manuscript received June 28, 2020; revised August 13, 2020; accepted September 17, 2020. Date of online publication December 21, 2020; date of current version April 9, 2022. This work was supported in part by the National Key R&D Program of China under Grant 2018YFE0208400, in part by the Zhejiang Provincial Natural Science Foundation of China under Grant LQ21E070003 and in part by the 2022 Open Foundation of National Key Laboratory "Coordinated Operation and Autonomous Planning of New Power Transmission and Distribution Systems Considering Source-Network-Load Uncertainties".

J. Liu is with the Department of Automation, Hangzhou Dianzi University, Hangzhou 310018, China, and also with the Department of Electrical Engineering, Zhejiang University, Hangzhou 310027, China.

P. L. Zeng (corresponding author, email: pingliangzeng@126.com; ORCID: 0000-0003-0590-0123) and H. Xing are with the Department of Automation, Hangzhou Dianzi University, Hangzhou 310018, China.

Y. L. Li is with the China Electric Power Research Institute, Beijing 100192, China.

Q. W. Wu is with the Department of Electrical Engineering, Technical University of Denmark, Kongens Lyngby 2800, Denmark.

DOI: 10.17775/CSEEJPES.2020.02860

$P_i^{\mathrm{DG,cur}}$, $Q_i^{\mathrm{DG,cur}}$ Active (MW) and reactive (Mvar) DG curtailments at bus $i$.

$P_i^{\mathrm{DG}}, Q_i^{\mathrm{DG}}$ Active (MW) and reactive (Mvar) powers provided by DGs at bus $i$.

$\varphi_i^{\mathrm{DG}}$ Power factor angle of DGs at bus $i$ (rad).

$P_{ij}, Q_{ij}$ Active (MW) and reactive (Mvar) power flows between buses $i$ and $j$.

$FP_{ij}$ Fictitious active power flow between buses $i$ and $j$ (MW).

$S_F^k$ Load of feeder section $F_k$ (MVA).

$k_{ij,t}$ OLTC tap position in period $t$.

$x_{\mathrm{s,sc,t}}$ Binary variable for switch status in scenario $sc$ and period $t$.

### C. Parameters

$N_{\mathrm{s}}^{\max}$ Upper limit of switching actions.

$k_{ij}^{\min}, k_{ij}^{\max}$ Lower and upper limits of OLTC tap position.

$\omega_{\mathrm{cur}}^{\max}$ Upper limit of DG curtailment rate.

$P_i^{\mathrm{DG,max}}$ Upper limit of active power provided by DGs at bus $i$ (MW).

$\varphi_i^{\mathrm{DG,min}}$, $\varphi_i^{\mathrm{DG,max}}$ Lower and upper limits of power factor angles of DGs at bus $i$ (rad).

$P_{i,\max}^{\mathrm{L,DSM}}$ Upper limit of active load that participates in DSM at bus $i$ (MW).

$U_i^{\min}, U_i^{\max}$ Lower and upper limits of voltage magnitude at bus $i$ (p.u.).

$I_{l,i}^{\max}$ Upper limit of current magnitude at branch $i$ (kA).

$\mathrm{SD}_k^{\min}$ Lower limit of SD of $F_k$ (MVA).

$\alpha_{h,k}$ Coefficient of $S_F^k$ in hyperplane $h$ (MVA $^{-1}$).

$p_{\mathrm{sc}}$ Probability of scenario $sc$.

$d_{\mathrm{sc,t}}$ Duration of configuration in scenario $sc$ and period $t$ (h).

$c^{\mathrm{s}}$ Cost of each switching ($).

$c_{\mathrm{sc,t}}^{\mathrm{p}}$ Electricity price in scenario $sc$ and period $t$ ($/MWh).

$c^{\mathrm{DSM}}$ DSM incentive cost ($/MWh).

$c_i^{\mathrm{WTG,OM}}$, $c_i^{\mathrm{PVG,OM}}$ Unit operation costs of WTGs and PVGs at bus $i$ ($/MWh).

$c_i^{\mathrm{WTG,AM}}$, $c_i^{\mathrm{PVG,AM}}$ Unit AM costs of WTGs and PVGs at bus $i$ ($/MWh).

$P_i^{\mathrm{L}}, Q_i^{\mathrm{L}}$ Active (MW) and reactive (Mvar) power demands at bus $i$.

$\varphi_i^{\mathrm{L}}$ Power factor angle of loads at bus $i$ (rad).

$r_{ij}, x_{ij}$ Resistance and reactance of branch $ij$ ($\Omega$).

$\Delta d$ Tap distance.

$M$ Large positive number.

$N_{\mathrm{bus}}$ Number of buses.

$N_{\mathrm{root}}$ Number of substation buses.

$N_{\mathrm{fdr}}$ Number of feeder sections.

$N_{\mathrm{sc}}$ Number of scenarios.

## I. Introduction

THE optimal operation problem for active distribution networks (ADNs) involves solving the optima for the decision variable set. The decision variables for the optimal operation problem are normally the tap position in the on-load tap-changers (OLTCs), the power injection by distributed generations (DGs), the power factor angle of DGs, the load participating in demand side management (DSM) and the status of switches. Here, the common DGs include gas turbine generators (GTGs), wind turbine generators (WTGs) and photovoltaic generators (PVGs), etc. Voltage rise and bi-directional power flow [1], [2] are two of the major impacts caused by rapid penetration of DGs in ADNs. As a result, active management (AM) becomes an effective tool for distribution network operators (DNOs) to mitigate these problems.

The stochastic optimization problem of operating ADN has a decision-making framework that can determine both discrete and continuous variables. When considering the uncertainty related to energy supply and demand, discrete variables and continuous variables should be determined at different stages [3], [4]. Specifically, setting discrete variables as the first-stage variables should be "determined here" before solving the continuous variables of the second-stage "waiting for observation" variables. These are typical two-stage recourse problems, which are usually expressed as a main problem together with sub-problems. Therefore, the objective function is divided into deterministic terms composed of discrete variables and random terms composed of continuous variables. By using scenarios to represent uncertainty, the optimization problem can be determined from the deterministic formula, and the expected value of the deterministic objective function can be minimized. The result is the weighted sum of the objective function that may realize the uncertainty and their respective probability of occurrence. Moreover, the decision variables of the upper-level problem are made under uncertainties. The decision variables of the lower-level problem (e.g., the output of each DG) are solved to guarantee the customer's power supply in each scenario. Thus, it is formulated the uncertainties associated with DG generation and load variation as the bi-level adaptive mixed-integer problem.

In general, operation optimization is formulated as a mixed integer nonlinear programming (MINLP) problem. In the specialized literature, a variety of approaches have been proposed to solve this NP-hard problem. These approaches involve heuristic and metaheuristic techniques, including dynamic programming [5], [6], genetic algorithms [7], [8], ant colony search algorithm [9], [10], evolutionary algorithms [11]–[13], etc. A multi-period optimal power flow (OPF) formulation for the minimum loss operation of distribution networks was proposed in [14] to obtain the optimal control schemes of capacitor banks, line switches and PVGs. Gabash and Li [15] presented a solution for active-reactive OPF in distribution networks with WTGs and battery storage. However, due to the time-varying profiles of DGs, demand and prices, the fixed charge and discharge periods for each day led to low-quality solutions. To make an improvement, Gabash and Li extended the above active-reactive OPF method by incorporating the flexible operation of battery storage systems [16]. In [17], a dynamic OPF formulation was developed to optimize the DGs, energy storage and flexible demand. Larimi *et al*. [18] proposed risk-based reconfiguration of ADNs by considering load

and generation uncertainty. The proposed method takes several forms of reward/penalty schemes in ADNs into account, but ignores many normal AM schemes, e.g., OLTC voltage regulation, DG curtailment, DG power factor control, and DSM. Generally speaking, normal AM schemes and network reconfiguration can both contribute to optimizing the operation of distribution networks, but most of the previous studies only consider them respectively or partially. Thus, the combination of normal AM schemes and network reconfiguration should be thoroughly proposed to achieve the optimal operation mode for a given distribution network.

The existing topological structures for distribution networks can be roughly divided into two major categories: radial and interconnected. However, the urban distribution networks tend to be interconnected in recent years. The interconnections among substation transformers supplies a transfer path for interrupt load demand when a substation transformer or a feeder faults. These interconnections assume that transformers in different substations are able to back up each other through the enhanced feeder network.

Furthermore, with the full benefits of distribution automation and measurement, remote switch regulation is much faster [19], [20] and feeder demand is detected by feeder terminal units [21]. These progresses make it quickly and flexibly available for power to transfer among adjacent substations through tie-switch actions [22]. Song *et al*. [23] designed two distribution management systems to make improvements in the flexibility and control of distribution networks. These two systems allowed loads to transfer among different substations by automatic sectionalizing switch operations after a transformer contingency. In [24], a straightforward evaluation method for power supply capability of distribution networks was proposed with the consideration of transformer contingencies. Junior *et al*. [25] presented a multi-objective multi-stage planning problem for distribution networks. The fault power restoration after a contingency was also integrated to improve system reliability. These studies show that the network transfer capability of distribution networks can postpone the upgrades and exploit the assets, while it has not been thoroughly considered in operation optimization. Since $N-1$ criterion is normally adopted as the basic guideline for system operations, the restored loads under contingencies cannot overload any component in the network when obtaining optimal operation solutions.

This paper presents an optimal operation model for ADNs formulated as a stochastic multi-objective dynamic MINLP problem. The proposed model considers OLTC voltage regulation, DG curtailment, DG power factor control, DSM and network reconfiguration simultaneously and is applicable to interconnected networks in general. In addition, the fault power affected by contingencies can be restored by line switching and the use of tie lines. $N-1$ security and the combination of normal boundary intersection (NBI) and dynamic niche differential evolution algorithm (DNDEA) are considered for operation modeling and optimization problem solving. The main contribution of this paper is to develop an optimal operation model for gas turbine integrated distribution networks considering AM schemes, which has the following advantages: 1) a flexible, secure and economic operation model. 2) with the full consideration of four controllable devices, including DGs, OLTCs, switches and interruptible demand. 3) trade-off between system operation economy and security.

The remainder of this paper is organized as follows. Section II describes the distance-based security assessment method under contingencies, Section III presents the proposed optimal operation model, Section IV outlines the simulation results of the model and Section V discusses the conclusions from these results.

## II. Distance-based Security Assessment Under Contingencies

The security assessment of distribution networks has been evolving from the traditional sequential $N-1$ contingency testing to a "quantitative analysis" approach, known as security distance (SD) [26]. According to the definition of SD, it can provide the exact security margin information for DNOs. Then, DNOs can adopt security control operations to guarantee the secure operation of distribution systems and to ensure systems operate at moderate levels in order to accommodate the large-scale uncertainties or even, contingencies. Thus, the distance-based security assessment methodology provides better efficiency and security of service under a well-designed algorithm.

First, some fundamental concepts are described in the following.

*a) N-1 security guideline:* The $N-1$ standard is the basic criterion for the operation of distribution systems. If one distribution network is $N-1$ secure, it indicates that all the load can be supplied with all the component capacity constraints satisfied when a single contingency occurs [26]. In urban areas, the non-supplied load is assumed to be transferred to different feeders and substations by line switching and the use of tie lines. Two contingency types, i.e., feeder contingency and transformer contingency, are fully proposed in this paper.

*b) Operating points:* In the distribution system, the operating point is the smallest set of state variables representing the $N-1$ security of the system, which can be as shown in [24]

$$W_f = \left(S_F^1, S_F^2, \cdots, S_F^k, \cdots S_F^n\right) \tag{1}$$

*c) Security region (SR):* The SR of the distribution network is defined as a set of operating points that ensure the $N-1$ security of the system [27]. When a feeder or substation transformer fails, the basic SR constraints are conductor capacity constraints and bus voltage constraints. Therefore, the SR model is formulated as

$$\Omega_{\mathrm{SR}} = \{W_f | g(W_f) \le 0\} \tag{2}$$

where $\Omega_{\mathrm{SR}}$ represents the SR. $g(W_f)$ is numbers of network security constraints after an $N-1$ contingency, which can be denoted as

$$\begin{cases} R_U = \{U \in R^{n-1} | U_i^{\min} \le U_i \le U_i^{\max},\ \forall i \in \Phi^{(b)}\} \\ R_I = \{I_1 \in R^{n-1} | 0 \le I_{l,i} \le I_{l,i}^{\max},\ \forall i \in \Phi^{(l)}\} \end{cases} \tag{3}$$

$R_U$ is the bus voltage constraint. $R_I$ is the branch current constraint, including the feeder capacity constraint and transformer capacity constraint.

*d) SR boundary:* For a certain distribution network, there is an SR boundary between secure and insecure operating points, which can be simulated by the $N-1$ approximation method. It has been demonstrated that the boundary is almost linear and thus can be illustrated by several hyperplanes [27]. Fig. 1 shows a two-dimension schematic diagram of SR, where two feeder loads are chosen as variables. The curve with solid dots represents the accurate boundary while the solid straight line corresponds to the linear boundary. The area surrounded by the boundaries is the SR. "•" is the secure operating point, "+" is the insecure operating point. Only secure points are in the SR, while others are not.

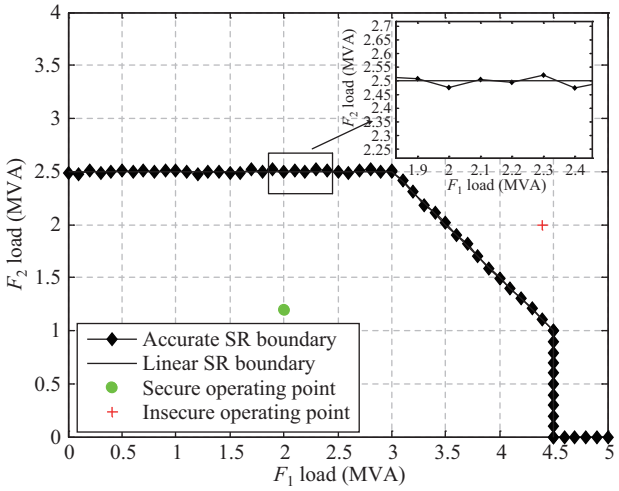


Fig. 1. Schematic diagram of SR.

From the concepts above, the location of the operating point can reflect the $N-1$ security of the distribution system. In order to quantitatively describe the security margins of system operations, the concept of SD is defined as the minimum distance from a specific operating point to any boundary of SR, which can be formulated as

$$\mathrm{SD}_k=\begin{cases}\min_{W_{f0}\in B_k}\|W_f-W_{f0}\|, \\ \qquad B_k\in\partial\Omega_{\mathrm{SR}}, W_f\in\Omega_{\mathrm{SR}} \\ -\min_{W_{f0}\in B_k}\|W_f-W_{f0}\|, \\ \qquad B_k\in\partial\Omega_{\mathrm{SR}}, W_f\notin\Omega_{\mathrm{SR}}\end{cases} \tag{4}$$

It is worthy to mention that, to improve the computational efficiency, $\mathrm{SD}_k$ is flexibly calculated using the algorithm in [28].

## III. Stochastic Multi-objective Model for Optimal Operations

### A. Problem Formulation

This subsection presents the proposed optimal operation problem formulation, where two objectives, expectation cost (EC) and Variation coefficient of SD (VCSD), as well as the constraints, power balance constraints, network security constraints and AM constraints, are considered. The set of decision variables of this optimization problem comprises the switch status, OLTC tap position, power provided by the DG, DG power factor angle and load participating in DSM. The DG types are GTGs, WTGs and PVGs in this paper. The wind speed and illumination intensity for each hour of the day are modeled as a scenario using historical data [29]–[31].

*1) EC*

In this paper, the EC is formulated as the sum of the switching cost, DG operation cost, DG AM cost, cost of energy purchasing from the upstream grid, loss cost and DSM cost. The mathematical expression is as follows

$$EC=\sum_{sc\in\Phi^{(sc)}}p_{\mathrm{sc}}\sum_{t\in\Phi^{(t)}}\begin{pmatrix}C^{\mathrm{S}}_{\mathrm{sc,t}}+C^{\mathrm{OM}}_{\mathrm{sc,t}}+C^{\mathrm{AM}}_{\mathrm{sc,t}}\\ +C^{\mathrm{P}}_{\mathrm{sc,t}}+C^{\mathrm{LOSS}}_{\mathrm{sc,t}}+C^{\mathrm{DSM}}_{\mathrm{sc,t}}\end{pmatrix} \tag{5}$$

where

$$C^{\mathrm{S}}_{\mathrm{sc,t}}=c^{\mathrm{s}}\left\{\sum_{s\in\Phi^{(s)}}\left\{\begin{matrix}x_{\mathrm{s,sc,t}}(x_{\mathrm{s,sc,t}}-x_{\mathrm{s,sc,t-1}})\\ +x_{\mathrm{s,sc,t-1}}(x_{\mathrm{s,sc,t-1}}-x_{\mathrm{s,sc,t}})\end{matrix}\right\}\right\} \tag{6}$$

$$C^{\mathrm{OM}}_{\mathrm{sc,t}}=d_{\mathrm{sc,t}}\sum_{i\in\Phi^{(d)}}\Big(c_i^{\mathrm{GTG,OM}}P^{\mathrm{GTG}}_{\mathrm{i,sc,t}}+c_i^{\mathrm{WTG,OM}}P^{\mathrm{WTG}}_{\mathrm{i,sc,t}} +c_i^{\mathrm{PVG,OM}}P^{\mathrm{PVG}}_{\mathrm{i,sc,t}}\Big) \tag{7}$$

$$C^{\mathrm{AM}}_{\mathrm{sc,t}}=d_{\mathrm{sc,t}}\sum_{i\in\Phi^{(d)}}\Big(c_i^{\mathrm{GTG,AM}}P^{\mathrm{GTG}}_{\mathrm{i,sc,t}}+c_i^{\mathrm{WTG,AM}}P^{\mathrm{WTG}}_{\mathrm{i,sc,t}} +c_i^{\mathrm{PVG,AM}}P^{\mathrm{PVG}}_{\mathrm{i,sc,t}}\Big) \tag{8}$$

$$C^{\mathrm{P}}_{\mathrm{sc,t}}=d_{\mathrm{sc,t}}c^{\mathrm{p}}_{\mathrm{sc,t}}P^{\mathrm{sub}}_{\mathrm{sc,t}} \tag{9}$$

$$C^{\mathrm{LOSS}}_{\mathrm{sc,t}}=d_{\mathrm{sc,t}}c^{\mathrm{p}}_{\mathrm{sc,t}}P^{\mathrm{loss}}_{\mathrm{sc,t}} \tag{10}$$

$$C^{\mathrm{DSM}}_{\mathrm{sc,t}}=d_{\mathrm{sc,t}}c^{\mathrm{DSM}}\sum_{i\in\Phi^{(b)}}P^{\mathrm{L,DSM}}_{\mathrm{i,sc,t}} \tag{11}$$

$C^{\mathrm{S}}_{\mathrm{sc,t}}, C^{\mathrm{OM}}_{\mathrm{sc,t}}, C^{\mathrm{AM}}_{\mathrm{sc,t}}, C^{\mathrm{P}}_{\mathrm{sc,t}}, C^{\mathrm{LOSS}}_{\mathrm{sc,t}}$ and $C^{\mathrm{DSM}}_{\mathrm{sc,t}}$ can be calculated by (6)–(11), respectively. $x_0$ corresponds to the original switch status for the first period.

*2) VCSD*

The VCSD is a defined security measure used to evaluate system security level under restoration after a contingency. It reflects the location of an operating point in SR, which can be used as a decision-making index in system security assessment from the real-time operation view. The VCSD is mathematically expressed as

$$\mathrm{VCSD}=\frac{1}{N_{\mathrm{sc}}}\sum_{sc\in\Phi^{(sc)}}\frac{\mathrm{SDSD_{sc}}}{\mathrm{EVSD_{sc}}} \tag{12}$$

where

$$\mathrm{EVSD_{sc}}=\frac{1}{N_{\mathrm{fdr}}}\sum_{k\in\Phi^{(f)}}\mathrm{SD_{k,sc}} \tag{13}$$

$$\mathrm{SDSD_{sc}}=\sqrt{\frac{1}{N_{\mathrm{fdr}}}\sum_{k\in\Phi^{(f)}}(\mathrm{SD_{k,sc}}-\mathrm{EVSD_{sc}})^2} \tag{14}$$

$\mathrm{EVSD_{sc}}$ and $\mathrm{SDSD_{sc}}$ can be formulated as (13) and (14), respectively.

*3) Objective functions*

The objectives for this optimal operation problem are to simultaneously minimize EC and VCSD, as shown in the following equation

$$\mathrm{Minimize(EC, VCSD)} \tag{15}$$

*4) Constraints*

The constraints must be satisfied in each period for all the scenarios. In the following equations except (27), the subscripts $sc$ and $t$ are all omitted.

*a) Active and reactive power balance constraints:*

$$\sum_{i\in\Phi^{(j)}}(P_{ij}-r_{ij}L_{ij})+P_j=0,\ \forall j\in\Phi^{(b)} \tag{16}$$

$$\sum_{i\in\Phi^{(j)}}(Q_{ij}-x_{ij}L_{ij})+Q_j=0,\ \forall j\in\Phi^{(b)} \tag{17}$$

$$\|2P_{ij}\ \ 2Q_{ij}\ \ L_{ij}-V_i\|_2^{\mathrm{T}}\le L_{ij}+V_i,\ \forall i\in\Phi^{(j)} \tag{18}$$

*b) Active and reactive power injection constraints:*

$$P_i=P_i^{\mathrm{DG}}-P_i^{\mathrm{DG,cur}}-P_i^{\mathrm{L}}+P_i^{\mathrm{L,DSM}},\ \forall i\notin\Phi^{(r)} \tag{19}$$

$$Q_i=Q_i^{\mathrm{DG}}-Q_i^{\mathrm{DG,cur}}-Q_i^{\mathrm{L}}+Q_i^{\mathrm{L,DSM}},\ \forall i\notin\Phi^{(r)} \tag{20}$$

*c) Branch equation constraints:*

$$V_i-V_j\le 2(r_{ij}P_{ij}+x_{ij}Q_{ij})-(r_{ij}^2+x_{ij}^2)L_{ij}+M(1-x_{\mathrm{s}}) \tag{21}$$

$$V_i-V_j\ge 2(r_{ij}P_{ij}+x_{ij}Q_{ij})-(r_{ij}^2+x_{ij}^2)L_{ij}-M(1-x_{\mathrm{s}}) \tag{22}$$

*d) Feeder SD limits [26]:*

$$\mathrm{SD}_k=\min_{h\in\Phi^{(k)}}\left\{\frac{1}{\alpha_{h,k}}-\frac{1}{\alpha_{h,k}}\sum_{\substack{l=1,\cdots,N_{\mathrm{fdr}}\\ l\neq k}}\alpha_{h,l}S_F^l\right\} \tag{23}$$

$$\mathrm{SD}_k\ge\mathrm{SD}_k^{\min},\ \forall k\in\Phi^{(f)} \tag{24}$$

*e) Node voltage limits:*

$$P\{U_i^{\min}\le U_i\le U_i^{\max}\}\ge\beta_U,\ \forall i\in\Phi^{(b)} \tag{25}$$

where $P\{\cdot\}$ denotes the probability of an incident in $\{\cdot\}$. $\beta$ is the specified probability to conduct the incident.

*f) Switch status constraint:*

$$x_{\mathrm{s}}\in\{0,1\},\ \forall s\in\Phi^{(s)} \tag{26}$$

*g) Switching action constraint between two periods:*

$$\sum_{s\in\Phi^{(s)}}\left\{\begin{matrix}x_{\mathrm{s,sc,t}}(x_{\mathrm{s,sc,t}}-x_{\mathrm{s,sc,t-1}})\\ +x_{\mathrm{s,sc,t-1}}(x_{\mathrm{s,sc,t-1}}-x_{\mathrm{s,sc,t}})\end{matrix}\right\}\le N_{\mathrm{s}}^{\max},$$
$$\forall sc\in\Phi^{(sc)},\ \forall t\in\Phi^{(t)} \tag{27}$$

This constraint depicts the fact that the DNO is not willing to change switch statuses by using more than $N_{\mathrm{s}}^{\max}$ actions between two periods for each scenario.

*h) Radiality constraints:*

$$\sum_{s\in\Phi^{(s)}}x_{\mathrm{s}}=N_{\mathrm{bus}}-N_{\mathrm{root}} \tag{28}$$

$$\sum_{j\in\Phi^{(i)}}FP_{ij}=-1,\ \forall i\notin\Phi^{(r)} \tag{29}$$

As testified to in [32], [33], constraints (28) and (16)–(22) ensure radiality in distribution networks. However, when there are some DGs or zero-injection buses, this conclusion may be insufficient. Thus, a practical solution is to add a fictitious power balance constraint for each bus, as shown in (29). When constraints (28) and (29) are satisfied, the bus is never isolated and the distribution network maintains a radial status for all the scenarios.

*i) OLTC voltage control constraints [34]:*

$$U_j=U_i(1+k_{ij,t}\Delta d),\ \forall ij\in\Phi^{(lt)},\ \forall t\in\Phi^{(t)} \tag{30}$$

$$k_{ij}^{\min}\le k_{ij,t}\le k_{ij}^{\max},\ \forall ij\in\Phi^{(lt)},\ \forall t\in\Phi^{(t)} \tag{31}$$

$$k_{ij,t}\in\{\text{integers}\},\ \forall ij\in\Phi^{(lt)},\ \forall t\in\Phi^{(t)} \tag{32}$$

$$\sum_{t=1}^{24}|\operatorname{sign}(k_{ij,t}-k_{ij,t-1})|\le 6,\ \forall ij\in\Phi^{(lt)},\ \forall t\in\Phi^{(t)} \tag{33}$$

The OLTC allows the positions of tap changers to be adjusted in discrete steps during the operation periods.

*j) DG curtailment constraints:*

$$(1-\omega_{\mathrm{cur}}^{\max})P_i^{\mathrm{DG,max}}\le P_i^{\mathrm{DG}}\le P_i^{\mathrm{DG,max}},\ \forall i\in\Phi^{(d)} \tag{34}$$

$$Q_i^{\mathrm{DG,cur}}=P_i^{\mathrm{DG,cur}}\tan\varphi_i^{\mathrm{DG}},\ \forall i\in\Phi^{(d)} \tag{35}$$

*k) DG power factor control constraint:*

$$\varphi_i^{\mathrm{DG,min}}\le\varphi_i^{\mathrm{DG}}\le\varphi_i^{\mathrm{DG,max}},\ \forall i\in\Phi^{(d)} \tag{36}$$

*l) DSM participation constraints:*

$$0\le P_i^{\mathrm{L,DSM}}\le P_{i,\max}^{\mathrm{L,DSM}},\ \forall i\in\Phi^{(b)} \tag{37}$$

$$Q_i^{\mathrm{L,DSM}}=P_i^{\mathrm{L,DSM}}\tan\varphi_i^{\mathrm{L}},\ \forall i\in\Phi^{(b)} \tag{38}$$

It is worthy to mention that the power factor of loads at each bus keeps constant when curtailing loads.

### *B. Implementation of NBI and DNDEA*

The optimal operation model is formulated as a stochastic multi-objective MINLP problem. To find an operation mode with minimum EC and VCSD, the combination of NBI and DNDEA is proposed in this paper. The main stages of the proposed algorithm are depicted in the flowchart of Fig. 2. The detailed technique and procedure of NBI method is described in [35]. Unlike the weighted sum method discussed in [36], the NBI algorithm takes advantage of scalarizing solutions that retain a good diversity in the criterion space. To extract a Pareto-optimal solution for DNOs, a fuzzy decision-making approach [37] is implemented to choose the best compromise solution.

The differential evolution algorithm (DEA) is a population-based stochastic search algorithm introduced by Storn and Price in 1995 [38]. Its main advantage is the ability to search the problem space globally and locally. The major stages of DEA have been introduced in [39], where an initial population of chromosomes is randomly generated by arbitrarily selecting "0" or "1" for each gene in a chromosome under the condition that each chromosome satisfies the problem constraints. If the operation mode does not meet the constraints, it would be deleted from the population, otherwise, the corresponding EC and VCSD for each chromosome are calculated until the convergence criteria is satisfied. To enhance the total search ability of the DEA and to avoid the premature convergence, a dynamic niche mechanism is deployed in this paper [40]. This method can estimate the optimal values for the population size and the niche radius without any a priori information on the fitness landscape based on an explicit identification of the peaks in the fitness landscape. It dynamically changes the niche radius by the following new two-stage annealing method

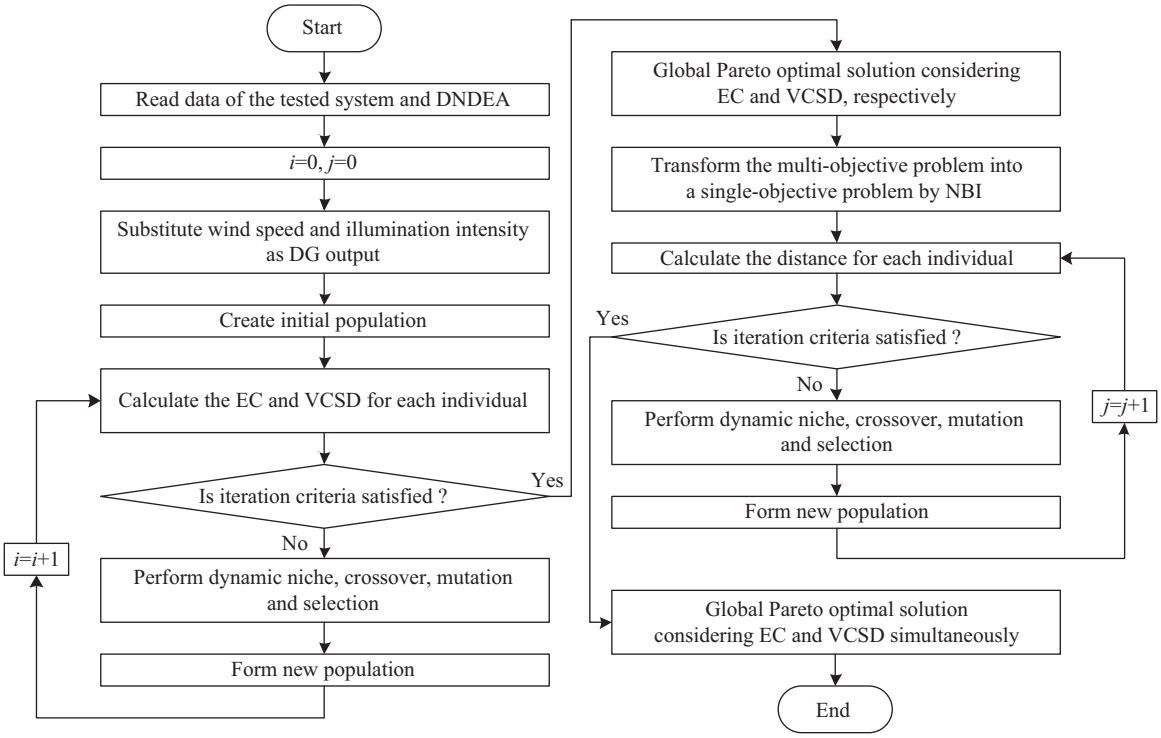


Fig. 2. Flowchart of the proposed optimization algorithm.

*a) First stage:* The exploration dominates the search process and the radius narrows in the speed of exponent as

$$r = r_{\text{initial}} as^{\text{h}} \tag{39}$$

where $h$ is the current iterations, $r_{\text{initial}}$ is the initial radius as shown in (40) and $as$ is a variable between 0 and 1 which is determined in (41)

$$r_{\text{initial}} = \frac{2\sum_{i=1}^{N_{\text{P}}-1}\sum_{j=i+1}^{N_{\text{P}}}\|x_i - x_j\|}{N_{\text{P}}(N_{\text{P}}-1)} \tag{40}$$

$$as = \left(\frac{r_{\text{cut}}}{r_{\text{initial}}}\right)^{\frac{1}{N_{\text{cut}}}} \tag{41}$$

where $N_{\text{P}}$ is the population size, $\|\cdot\|$ is the Euclidean distance between the two vectors $x_i$ and $x_j$. $r_{\text{cut}}$ is the distance bound value before turning to the second stage. $N_{\text{cut}}$ is the cut-off number of iterations before turning to the second stage, which is one third of the iterations in this paper.

*b) Second stage:* Set the radius as a constant and conduct the exploitation to improve the quality of the optimal value obtained. When the niche radius is greater than $r_{\text{cut}}$, the radius equals $r$. Otherwise, the radius equals $r_{\text{cut}}$.

## IV. Simulation Results

### A. Modified 104-bus Distribution Network

The proposed model is first tested on a modified 104-bus distribution network. The topology of the test system is shown in Fig. 3. More parameters of the initial network can be obtained from [41]. With no changes in the capacity and load of the existing transformers, the distribution network expands the initial network from 7 to 20 feeders and 38 to 104 demand sides. To configure an interconnected distribution network, seven more tie lines are constructed. The load types in this case are residential, industrial and commercial. Four GTGs are installed at buses 7, 30, 54 and 84, four WTGs are installed at buses 7, 31, 56 and 85, and two PVGs are installed at buses 10 and 38. The daily profiles of wind speed, illumination intensity and load demand are illustrated in Fig. 4. The simulation parameters are listed in Tables I–III. The proposed model is simulated using MATLAB R2013a in a personal computer

TABLE I
Data of OLTCs and Branches

| Substation | OLTC | OLTC capacity (MVA) | Branch capacity (MVA) | Unit resistance (Ω/km) | Unit reactance (Ω/km) |
|---|---|---|---|---|---|
| SP1 | 1 | 12.8 | 6.91 | 0.17 | 0.365 |
| | 2 | 12.8 | 6.91 | 0.17 | 0.365 |
| SP2 | 3 | 12.8 | 6.91 | 0.17 | 0.365 |
| | 4 | 12.8 | 6.91 | 0.17 | 0.365 |
| SP3 | 5 | 8.0 | 5.83 | 0.22 | 0.366 |
| | 6 | 8.0 | 5.83 | 0.22 | 0.366 |

TABLE II
Data of Load Demands

| Load demand | Load (MVA) | Type |
|---|---|---|
| 1–4, 18–20, 32, 44–47, 68, 94 | 0.444 | residential |
| 11–13, 33–36, 51–53, 57–59, 63–65, 69–71, 95–97, 99, 100 | 0.296 | residential |
| 48, 49, 72, 73, 98, 101 | 0.407 | industrial |
| 14, 15, 21–23, 37, 54, 60–62, 102, 103 | 0.271 | industrial |
| 8–10, 29, 43, 90 | 0.815 | residential |
| 26–28, 74–88, 91, 92 | 0.326 | residential |
| 30, 31, 39–42, 89, 93 | 0.611 | commercial |
| 5–7, 16, 17, 24, 25, 38, 50, 55, 56, 66, 67, 104 | 0.336 | commercial |

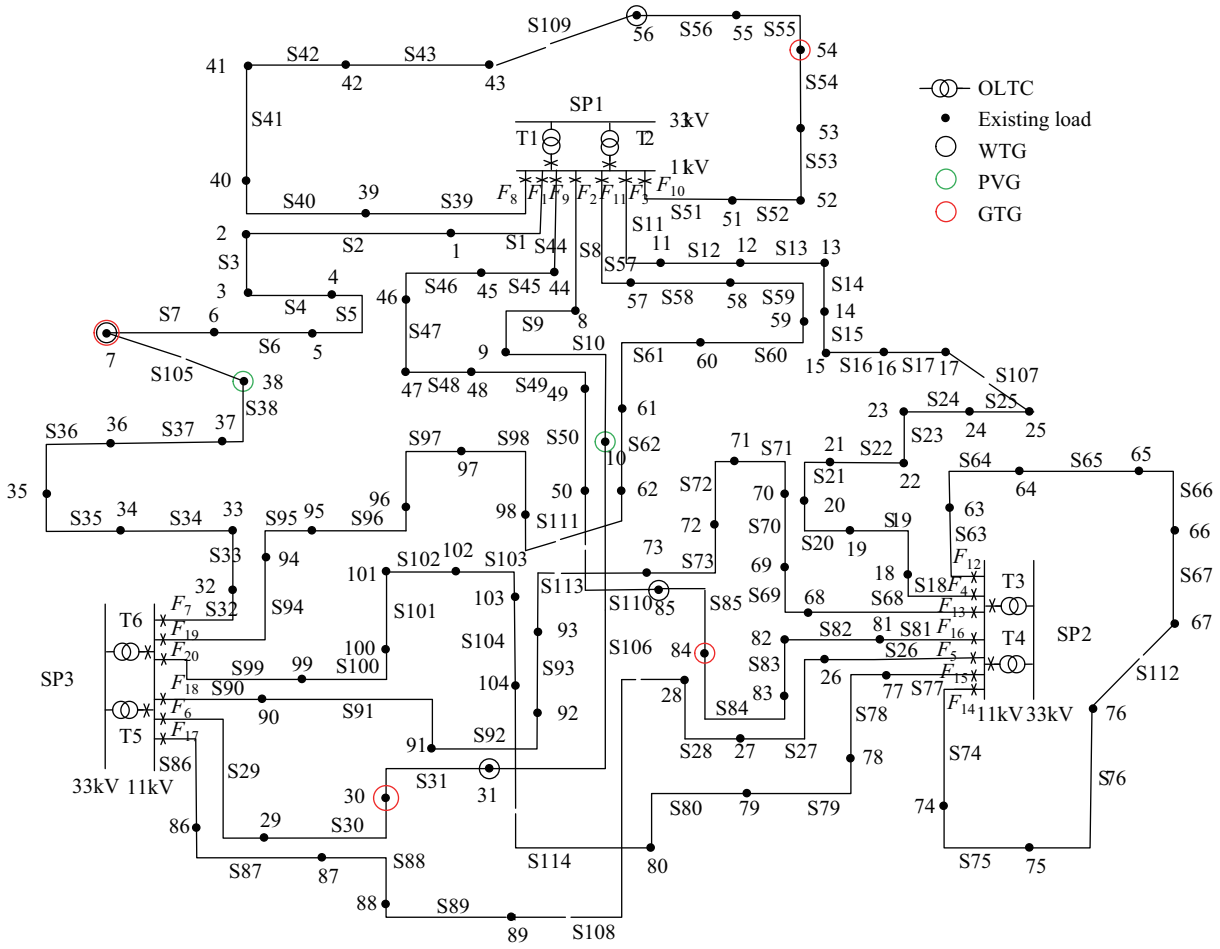


Fig. 3. Modified 104-bus distribution network.

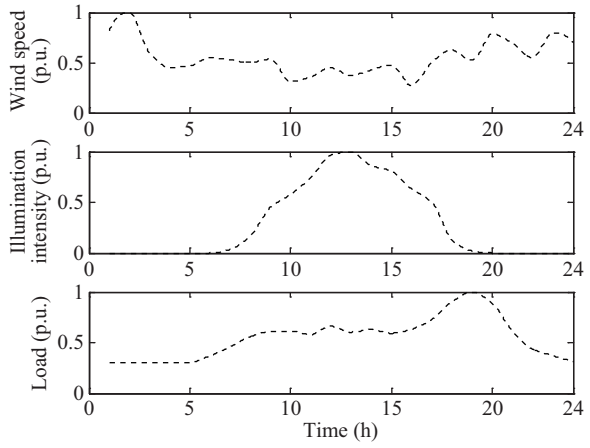


Fig. 4. Daily curve of wind speed, illumination intensity and load demand.

with 3.6 GHz CPU and 8 GB RAM.

In this study, four cases for the different parameter values of $SD_k^{min}$ are considered as follows:

Case 1: The system $N-1$ security is not considered in this case (i.e., there is no specified limits in the values of $SD_k^{min}$).

Case 2: The system $N-1$ security is just guaranteed in this case (i.e., the value of $SD_k^{min}$ is 0).

Case 3: The system is tested at medium security levels. In this case, $SD_k^{min}$ is considered as 0.15 MVA.

Case 4: The system is tested at high security levels. $SD_k^{min}$ is 0.3 MVA in this case.

Figure 5 shows the Pareto fronts obtained using the NBI

TABLE III
SIMULATION PARAMETER

| Parameter | Value |
|---|---|
| Unit DG capacity | 0.5 MW |
| Cut-in/rated/cut-out wind speed | 3, 13, 20 m/s |
| Rated illumination intensity | 0.5 kW/m$^2$ |
| GTG operation cost | 60 $/MW·h |
| GTG AM cost | 15 $/MW·h |
| WTG operation cost | 30 $/MW·h |
| WTG AM cost | 22.5 $/MW·h |
| PVG operation cost | 40 $/MW·h |
| PVG AM cost | 30 $/MW·h |
| Switching cost | 200 $/switching |
| DSM incentive price | 350 $/MW·h |
| Bus voltage bound | 0.95 p.u.–1.05 p.u. |
| OLTC secondary voltage | 0.95 p.u.–1.05 p.u. |
| DG curtailment rate | 0–50% |
| DG power factor | 0.98 (lagging)–0.98 (leading) |
| DSM participation rate | 0–1 p.u. |
| Iterations | 50 |
| Population | 50 |
| Scaling factor/crossover probability | 0.9–0.1 (linearly decreasing) |
| Electricity price | 70 $/MW·h (6:00 to 21:00) 35 $/MW·h (other time) |

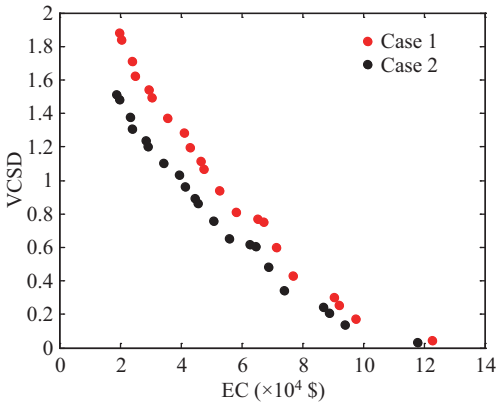


Fig. 5. Pareto fronts distribution for Cases 1 and 2.

method for Cases 1 and 2. As expected, EC is inversely proportional to VCSD. For example, in Case 1, the EC and VCSD are \$19,688 and 1.88, respectively, which denotes the lowest security at the lowest cost. However, the EC and VCSD are \$122,603 and 0.04, respectively, which represents the highest security at the highest cost. It can also be seen that the NBI method provides a set of uniformly distributed non-dominated solutions regardless of the scales of objective function values. Moreover, as shown in Fig. 5, the Pareto front outcomes for Case 2 are better than Case 1 with respect to the two objectives (i.e., EC and VCSD). Thus, it is worth mentioning that $N-1$ security should be thoroughly considered when selecting the optimal operation mode for the DNOs.

For benchmarking purposes, the optimal operation mode for Case 1 is illustrated in Fig. 6, which shows the tap positions of the OLTC T5, the active power generated by the DG at bus 31, the active power demand at bus 31 and the voltage profile of the bus 31 over a 24-h period. Fig. 6(a) shows that the taps of OLTC T5 are adjusted four times during one day. Moreover, it can be seen that, in order to satisfy node voltage limits, the tap position of OLTC T5 is adjusted lower when the load is light and the active power injected by the DG at bus 31 is high (e.g., between 1:00 and 2:00 A.M.) and adjusted higher when the load is heavy and the active power injected by the DG at bus 31 is low (e.g., between 15:00 and 16:00 P.M.). Fig. 6(b) shows that the active power injected by the DG at bus 31 is curtailed between 24:00 P.M. and 2:00 A.M. The reason can be explained as follows. The original active power injected by the DG at bus 31 is high while the load at bus 31 is low between 24:00 P.M. and 2:00 A.M. In order to be within the maximum voltage limit, for the DG at bus 31, the original active power decreases to the actual active power without adjusting the tap position of OLTC T5. Fig. 6(c) shows that the load at bus 31 is curtailed at 16:00 P.M when the active power injected by the DG at bus 31 is low. Due to the minimum voltage limit, the original load at bus 31 reduces to the actual load with adjusting the tap position of OLTC T5 to its maximum limit. Fig. 6(d) shows that all voltages at bus 31 are within their limits during one day.

As a contrast, the optimal operation solutions for Case 2 are shown in Fig. 7, which contains the same information as Fig. 6. In addition to the same conclusions drawn from

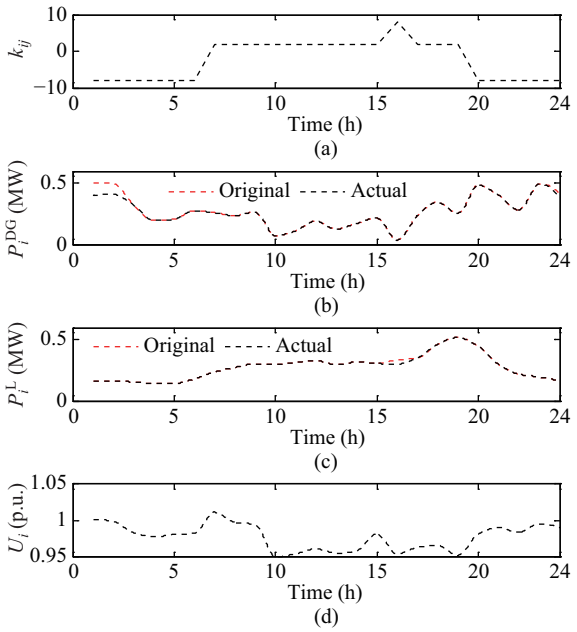


Fig. 6. Optimal operation of the 104-bus distribution system without considering $N-1$ security (Case 1). (a) Tap movements of the OLTC T5. (b) Active power injected by the DG at bus 31. (c) Active power demand at bus 31. (d) Voltage profile of the bus 31.

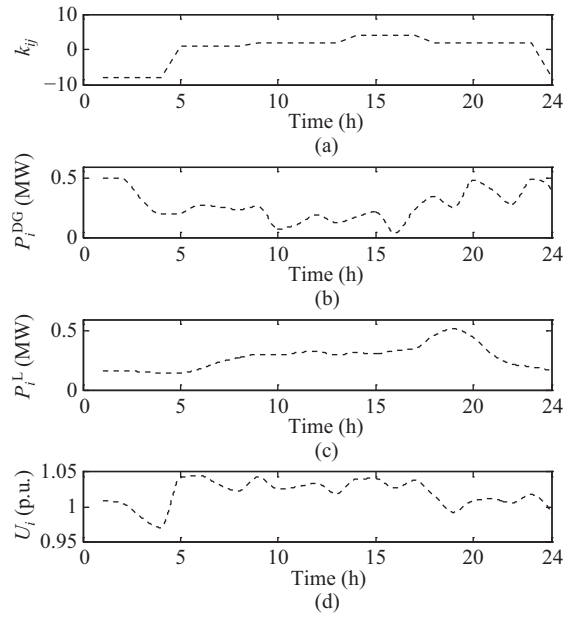


Fig. 7. Optimal operation of the 104-bus distribution system when considering $N-1$ security and $SD_k^{min}=0$ (Case 2). (a) Tap movements of the OLTC T5. (b) Active power injected by the DG at bus 31. (c) Active power demand at bus 31. (d) Voltage profile of the bus 31.

Fig. 6, the taps of OLTC T5 are adjusted five times over a 24-h period, as shown in Fig. 7(a). Likewise, all voltages at bus 31 are within their ranges, as shown in Fig. 7(d). It is worth mentioning that, in Case 2, there is no demand to curtail any load or active power injected by the DG at bus 31, as shown in Fig. 7(b) and (c). Thus, comparing to Case 1, the operation solution considering $N-1$ security (Case 2) improves the DG penetration level and better satisfies the power supply demand.

TABLE IV
OPTIMAL HOURLY FEEDER RECONFIGURATION FOR CASE 1

| Hour | Open switch | Hour | Open switch |
|---|---|---|---|
| 1, 24 | 105-106-25-108-56-50-62-66-73-104 | 13 | 38-10-107-89-43-50-62-66-73-114 |
| 2, 3 | 105-106-25-89-56-50-62-66-73-104 | 14, 15 | 38-10-107-89-43-50-98-66-73-114 |
| 4 | 105-106-25-89-56-50-62-66-73-114 | 16 | 38-106-107-89-43-50-98-66-73-114 |
| 5, 6 | 7-106-25-89-56-50-62-66-73-114 | 17 | 38-106-107-89-43-110-98-66-73-114 |
| 7 | 7-106-107-89-56-50-62-66-73-114 | 18 | 38-106-25-89-43-110-98-66-73-114 |
| 8 | 7-106-107-89-109-50-62-66-73-114 | 19 | 38-106-25-89-43-110-98-66-73-80 |
| 9 | 7-10-107-89-109-50-62-66-73-114 | 20 | 38-106-25-89-43-110-98-112-73-80 |
| 10 | 7-10-107-89-109-50-62-66-113-114 | 21 | 38-106-25-108-43-110-98-112-73-104 |
| 11 | 7-10-107-89-43-50-62-66-113-114 | 22 | 105-106-25-108-43-110-62-112-73-104 |
| 12 | 38-10-107-89-43-50-62-66-113-114 | 23 | 105-106-25-108-56-110-62-66-73-104 |

TABLE V
OPTIMAL HOURLY FEEDER RECONFIGURATION FOR CASE 2

| Hour | Open switch | Hour | Open switch |
|---|---|---|---|
| 1 | 38-30-21-108-54-47-61-65-93-101 | 15 | 7-31-21-28-56-47-111-65-93-80 |
| 2, 3 | 38-30-21-108-54-47-111-65-93-101 | 16 | 7-31-21-28-109-47-111-65-93-80 |
| 4 | 38-31-21-108-54-47-111-65-93-101 | 17, 18 | 7-31-21-28-109-47-62-65-93-80 |
| 5, 6 | 38-31-21-108-56-47-111-65-93-101 | 19 | 7-30-21-28-109-47-62-65-93-80 |
| 7-9 | 105-31-21-108-56-47-111-65-93-101 | 20 | 7-30-21-28-109-48-62-65-93-80 |
| 10 | 105-31-21-89-56-47-111-65-93-103 | 21 | 38-30-21-28-109-48-62-65-93-80 |
| 11, 12 | 105-31-21-28-56-47-111-65-93-103 | 22 | 38-30-21-28-54-48-62-65-93-101 |
| 13, 14 | 105-31-21-28-56-47-111-65-93-80 | 23, 24 | 38-30-21-108-54-48-61-65-93-101 |

Tables IV and V show the open switches of the hourly reconfiguration. There are 46 and 38 switching actions for Cases 1 and 2, respectively. This large number of switching actions is reduced by considering $N-1$ security. Furthermore, it is easy to see that considering $N-1$ security impacts the optimal configuration. Comparing Cases 1 and 2, we can see that the optimal configuration has been changed in all security levels and hours. This is because, in this paper, the optimal configuration is determined for the purpose of cost reduction and security improvement. As a result, the optimal configuration is quite affected as expected.

The information of SD for Cases 1 and 2 is shown in Fig. 8. It can be seen that, for each case, the SD of each feeder is different. This is because the SD of each feeder is simultaneously determined by the capacities of the transformer and feeder, the load of the feeder and the active power injected by the DG on the feeder. The results in Fig. 8 also indicates that operation solutions affect the value of SD. For instance, for Cases 1 and 2, the SD of feeders 2, 6 and 7 remarkably changes while the SD of feeders 12, 14 and 15 almost remains constant. The reason can be explained as follows. In this paper, the topology of the test system is an interconnected form.

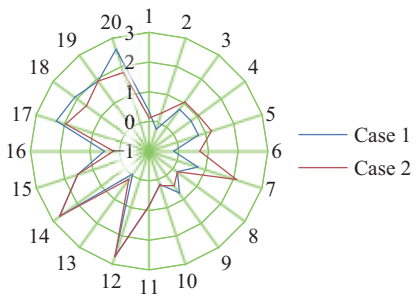


Fig. 8. SD of twenty feeders for Cases 1 and 2.

When the capacity of the feeder is small, $N-1$ security is determined only by the feeder capacity constraint and the SD changes slightly after network reconfiguration. However, when the capacity of the feeder is large, $N-1$ security is simultaneously determined by capacity constraints of the feeder and substation transformer and the SD changes a lot after feeder reconfiguration. Furthermore, the SD of feeders 2, 6 and 13 in Case 2 becomes positive in terms of Case 1. This indicates that the system $N-1$ security is guaranteed in Case 2.

The results of the optimal operation for Cases 1–4 are shown in Table VI, which includes EC, VCSD and the costs of the DG operation, energy purchase, power loss and DSM. As shown in Table VI, comparing the solutions of Cases 1 and 2, the economies of EC and VCSD obtained are 3.75% and 19.15%, respectively, when $N-1$ security is considered in optimizing system operations. This indicates that considering $N-1$ security can achieve securer operation solutions at lower cost. With increasing the minimum SD limit to 0.15 MVA (Case 3), the economies of EC and VCSD achieved are 1.35% and 31.91%, respectively, when compared with Case 1. However, when the minimum SD limit is increased to 0.3 MVA (Case 4), the operation solutions are infeasible. This is because the SD violations cannot be eliminated by the combination of OLTC voltage regulation, DG curtailment, DG power factor

TABLE VI
RESULTS OF THE OPTIMAL OPERATION FOR THE MODIFIED 104-BUS CASE

| Case | 1 | 2 | 3 | 4 |
|---|---|---|---|---|
| EC ($) | 52,802.3 | 50,820.8 | 52,088.3 | – |
| DG operation cost ($) | 1,284.5 | 1,329.6 | 1,315.2 | – |
| Energy purchase cost ($) | 38,104.0 | 37,977.6 | 38,302.3 | infeasible |
| Power loss cost ($) | 865.5 | 863.4 | 1,148.2 | – |
| DSM cost ($) | 2,385.1 | 2,053.1 | 2,136.2 | – |
| VCSD | 0.94 | 0.76 | 0.64 | – |

control, DSM and network reconfiguration, that is, although the flexibility of source-network-load is fully considered to regulate the system operation security, the optimal solution cannot be found under this circumstance since the security level is set too high. Moreover, although the DG operation cost increases in Case 2, the increased DG penetration and decreased DSM participation reduce the system power loss cost and energy purchase cost. The DNO can select each of the solutions considering the accepted security. Case 2 is superior to others when the DNO is security neutral due to its lowest EC. However, the security averse DNO selects Case 3 due to its highest security.

Under the same parameters and input conditions, the proposed DNDEA is compared with DEA, particle swarm optimization (PSO) [42], [43] and the genetic algorithm (GA) in the presence of optimization accuracy and efficiency, as shown in Table VII. As a benchmark, IPOPT [44] is also implemented to solve the optimal solution of Case 2. It can be noted that the DNDEA outperforms DEA, PSO and GA in reducing the EC, VCSD, iterations and computation time. This implies that the proposed algorithm can find higher quality solutions with excellent robustness, consistency and convergence properties. Furthermore, the deviation between the minimum EC obtained by DNDEA and IPOPT is 0.06%, which is acceptable. This indicates that the proposed DNDEA can guarantee the optimality of the operation solution.

TABLE VII
CONVERGENCE CHARACTERISTICS OF DIFFERENT ALGORITHMS FOR CASE 2

| Algorithm | DNDEA | DEA | PSO | GA | IPOPT |
|---|---|---|---|---|---|
| Minimum EC ($) | 50,820.8 | 50,872.5 | 50,905.4 | 50,910.1 | 50,789.2 |
| Mean EC ($) | 50,975.9 | 52,261.4 | 52,425.9 | 53,427.1 | — |
| Minimum VCSD | 0.76 | 0.77 | 0.77 | 0.78 | 0.76 |
| Mean VCSD | 0.77 | 0.79 | 0.80 | 0.81 | — |
| Mean iterations | 22.6 | 31.2 | 32.3 | 38.4 | — |
| Mean computation time (s) | 436.8 | 554.5 | 571.4 | 678.0 | 169.6 |

It should be emphasized that the best operating model is flexible, because the maximum limit of operating changes for each device is adjustable. Therefore, if a solution is needed that requires all controls to be appropriately adjusted within a period of time, the proposed model can accommodate this control.

### *B. A Real Urban Distribution Network*

The proposed model is further tested on a real urban distribution network in East China. Fig. 9 shows the diagram of the test system. The distribution network encompasses 3 substations, 6 transformers, 10 feeders and 73 load buses. WTGs are installed at buses 7, 22, 42, 61 and 70 with the total capacity of 4.8 MW and PVGs are allocated at buses 15, 23, 52 and 55 with the total capacity of 1.5 MW. The total capacity of GTGs at buses 12 and 37 is 2.0 MW. The peak load of this system is 60 MW.

For Cases 1 and 2, the operation results for this system are listed in Table VIII. As shown, the EC for Case 2 is reduced compared with that for Case 1. This indicates that Case 2 has better economic benefits than Case 1. Moreover, the VCSD for Case 2 is also smaller than that for Case 1, which reveals that, with the consideration of security constraints, the system security level can be significantly improved. In addition, the network flexibility can contribute to accommodating more DGs. Thus, the energy purchase cost and power loss cost are both reduced at the same DSM participation rate. All of the above further verify the generality of the proposed model and the applied algorithm.

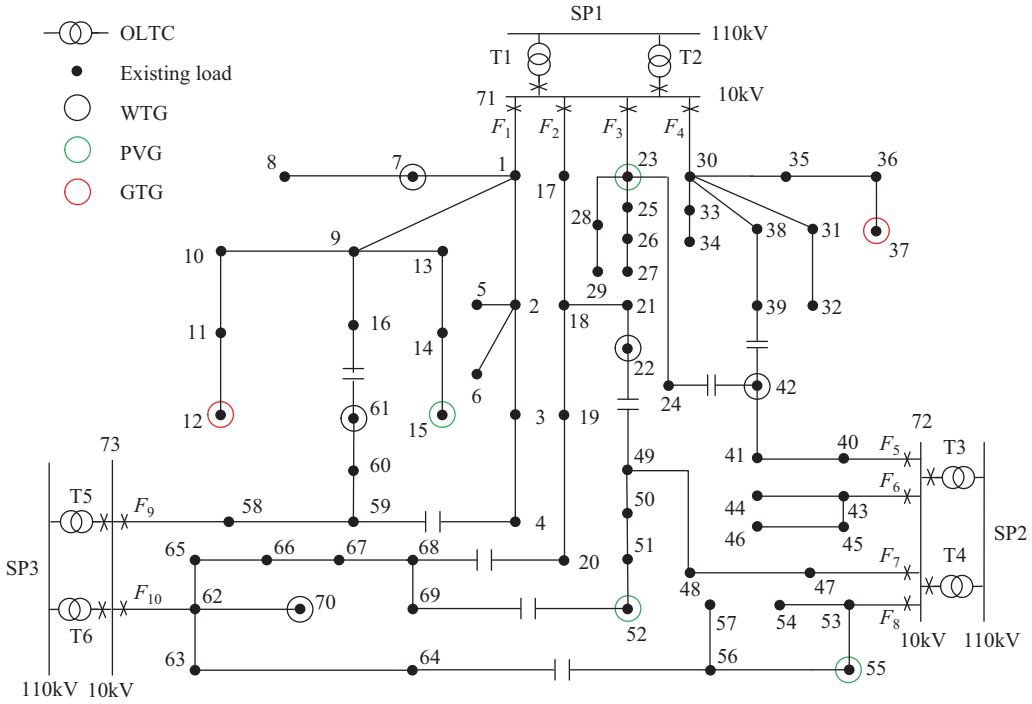


Fig. 9. A real urban distribution network.

TABLE VIII
RESULTS OF THE OPTIMAL OPERATION FOR THE REAL URBAN CASE

| Case | 1 | 2 |
|---|---|---|
| EC ($\times$ $10^4$ ¥) | 96.79 | 92.98 |
| DG operation cost ($\times$ $10^4$ ¥) | 2.35 | 2.41 |
| Energy purchase cost ($\times$ $10^4$ ¥) | 80.39 | 78.05 |
| Power loss cost ($\times$ $10^4$ ¥) | 0.80 | 0.75 |
| DSM cost ($\times$ $10^4$ ¥) | 0 | 0 |
| VCSD | 0.53 | 0.48 |

## V. CONCLUSION

This paper presents a stochastic MINLP model for solving the problem of optimal operation of gas turbine integrated distribution networks, which can guarantee system $N-1$ security. The proposed model considers DGs, tap-changers, load and switches as controllable devices. The objective is to simultaneously minimize the EC and VCSD. The steady-state operation of the flexible distribution network is modeled through the use of chance-constrained expressions. The formulated problem is solved via the techniques of NBI and DNDEA.

Numerical tests are carried out to demonstrate the advantages of the mathematical models and the efficiency of the proposed solution techniques. The results show that it is possible to determine the optimal operation solutions for gas turbine integrated distribution networks in the presence of AM schemes using a flexible, secure and economic MINLP model. The operation mode, considering $N-1$ security, can achieve significant losses in DG curtailment, load shedding and switching actions when compared to the solution without considering $N-1$ security. The DNO can select optimal operation solutions based on acceptable security. Due to the significant optimizability of the proposed model and its moderate computational burden, this method can be used as a basic analysis tool for scheduling system operation.

## REFERENCES


[1] H. J. Xing, H. Fan, X. Sun, S. Y. Hong, and H. Z. Cheng, "Optimal siting and sizing of distributed renewable energy in an active distribution network," *CSEE Journal of Power and Energy Systems*, vol. 4, no. 3, pp. 380–387, Sep. 2018.

[2] J. Yu, Y. Guo, and H. B. Sun, "Testbeds for integrated transmission and distribution networks: generation methodology and benchmarks," *CSEE Journal of Power and Energy Systems*, vol. 6, no. 3, pp. 518–527, Sep. 2020.

[3] H. Quan, D. Srinivasan, A. M. Khambadkone, and A. Khosravi, "A computational framework for uncertainty integration in stochastic unit commitment with intermittent renewable energy sources," *Applied Energy*, vol. 152, pp. 71–82, Aug. 2015.

[4] J. Liu, P. P. Zeng, H. Xing, Y. L. Li, and Q. W. Wu, "Hierarchical duality-based planning of transmission networks coordinating active distribution network operation," *Energy*, vol. 213, pp. 118488, Dec. 2020.

[5] Z. Wu, P. L. Zeng, and X. P. Zhang, "Two-stage stochastic dual dynamic programming for transmission expansion planning with significant renewable generation and $N$-$k$ criterion," *CSEE Journal of Power and Energy Systems*, vol. 2, no. 1, pp. 3–10, Mar. 2016.

[6] B. X. Liu, C. T. Cheng, S. Wang, S. L. Liao, K. W. Chau, X. Y. Wu, and W. D. Li, "Parallel chance-constrained dynamic programming for cascade hydropower system operation," *Energy*, vol. 165, pp. 752–767, Dec. 2018.

[7] T. W. Cui, W. Z. Zhao, and C. Y. Wang, "Design optimization of vehicle EHPS system based on multi-objective genetic algorithm," *Energy*, vol. 179, pp. 100–110, Jul. 2019.

[8] I. H. Sin and B. Do Chung, "Bi-objective optimization approach for energy aware scheduling considering electricity cost and preventive maintenance using genetic algorithm," *Journal of Cleaner Production*, vol. 244, pp. 118869, Jan. 2020.

[9] Y. B. Li, H. Soleimani, and M. Zohal, "An improved ant colony optimization algorithm for the multi-depot green vehicle routing problem with multiple objectives," *Journal of Cleaner Production*, vol. 227, pp. 1161–1172, Aug. 2019.

[10] L. K. Hu, Y. Liu, N. Lohse, R. Z. Tang, J. X. Lv, C. Peng, and S. Evans, "Sequencing the features to minimise the non-cutting energy consumption in machining considering the change of spindle rotation speed," *Energy*, vol. 139, pp. 935–946, Nov. 2017.

[11] P. P. Biswas, P. N. Suganthan, and G. A. J. Amaratunga, "Decomposition based multi-objective evolutionary algorithm for windfarm layout optimization," *Renewable Energy*, vol. 115, pp. 326–337, Jan. 2018.

[12] M. Ehteram, H. Karami, S. F. Mousavi, S. Farzin, and O. Kisi, "Optimization of energy management and conversion in the multi-reservoir systems based on evolutionary algorithms," *Journal of Cleaner Production*, vol. 168, pp. 1132–1142, Dec. 2017.

[13] X. H. Yuan, B. Q. Zhang, P. T. Wang, J. Liang, Y. B. Yuan, Y. H. Huang, and X. H. Lei, "Multi-objective optimal power flow based on improved strength Pareto evolutionary algorithm," *Energy*, vol. 122, pp. 70–82, Mar. 2017.

[14] R. A. Jabr, "Minimum loss operation of distribution networks with photovoltaic generation," *IET Renewable Power Generation*, vol. 8, no. 1, pp. 33–44, Jan. 2014.

[15] A. Gabash and P. Li, "Active-reactive optimal power flow in distribution networks with embedded generation and battery storage," *IEEE Transactions on Power Systems*, vol. 27, no. 4, pp. 2026–2035, Nov. 2012.

[16] A. Gabash and P. Li, "Flexible optimal operation of battery storage systems for energy supply networks," *IEEE Transactions on Power Systems*, vol. 28, no. 3, pp. 2788–2797, Aug. 2013.

[17] S. Gill, I. Kockar, and G. W. Ault, "Dynamic optimal power flow for active distribution networks," *IEEE Transactions on Power Systems*, vol. 29, no. 1, pp. 121–131, Jan. 2014.

[18] S. M. M. Larimi, M. R. Haghifam, and A. Moradkhani, "Risk-based reconfiguration of active electric distribution networks," *IET Generation, Transmission & Distribution*, vol. 10, no. 4, pp. 1006–1015, Mar. 2016.

[19] M. Sedighizadeh, R. V. Doyran, and A. Rezazadeh, "Optimal simultaneous allocation of passive filters and distributed generations as well as feeder reconfiguration to improve power quality and reliability in microgrids," *Journal of Cleaner Production*, vol. 265, pp. 121629, Aug. 2020.

[20] X. L. Fang, S. H. Ma, Q. Yang, and J. T. Zhang, "Cooperative energy dispatch for multiple autonomous microgrids with distributed renewable sources and storages," *Energy*, vol. 99, pp. 48–57, Mar. 2016.

[21] J. Xiao, G. Q. Zu, Y. Wang, X. S. Zhang, and X. Jiang, "Model and observation of dispatchable region for flexible distribution network," *Applied Energy*, vol. 261, pp. 114425, Mar. 2020.

[22] D. M. Staszesky, D. Craig, and C. Befus, "Advanced feeder automation is here," *IEEE Power and Energy Magazine*, vol. 3, no. 5, pp. 56–63, Sep./Oct. 2005.

[23] I. K. Song, S. Y. Yun, S. C. Kwon, and N. H. Kwak, "Design of smart distribution management system for obtaining real-time security analysis and predictive operation in Korea," *IEEE Transactions on Smart Grid*, vol. 4, no. 1, pp. 375–382, Mar. 2013.

[24] F. Z. Luo, C. S. Wang, J. Xiao, and S. Y. Ge, "Rapid evaluation method for power supply capability of urban distribution system based on $N$-1 contingency analysis of main-transformers," *International Journal of Electrical Power & Energy Systems*, vol. 32, no. 10, pp. 1063–1068, Dec. 2010.

[25] B. R. P. Junior, A. M. Cossi, J. Contreras, and J. R. S. Mantovani, "Multiobjective multistage distribution system planning using tabu search," *IET Generation, Transmission & Distribution*, vol. 8, no. 1, pp. 35–45, Jan. 2014.

[26] J. Liu, H. Z. Cheng, P. L. Zeng, and L. Z. Yao, "Rapid assessment of maximum distributed generation output based on security distance for interconnected distribution networks," *International Journal of Electrical Power & Energy Systems*, vol. 101, pp. 13–24, Oct. 2018.

[27] G. Q. Zu, J. Xiao, and K. Sun, "Mathematical base and deduction of security region for distribution systems with DER," *IEEE Transactions on Smart Grid*, vol. 10, no. 3, pp. 2892–2903, May 2019.

[28] S. J. Chen, Q. X. Chen, Q. Xia, and C. Q. Kang, "Steady-state security assessment method based on distance to security region boundaries," *IET Generation, Transmission & Distribution*, vol. 7, no. 3, pp. 288–297, Mar. 2013.
[29] X. L. Liu, Y. B. Liu, J. Y. Liu, Y. Xiang, and X. D. Yuan, "Optimal planning of AC-DC hybrid transmission and distributed energy resource system: Review and prospects," *CSEE Journal of Power and Energy Systems*, vol. 5, no. 3, pp. 409–422, Sep. 2019.
[30] G. R. Ren, J. Wan, J. F. Liu, D. R. Yu, and L. Söder, "Analysis of wind power intermittency based on historical wind power data," *Energy*, vol. 150, pp. 482–492, May 2018.
[31] J. Liu, H. Z. Cheng, P. L. Zeng, L. Z. Yao, C. Shang, and Y. Tian, "Decentralized stochastic optimization based planning of integrated transmission and distribution networks with distributed generation penetration," *Applied Energy*, vol. 220, pp. 800–813, Jun. 2018.
[32] M. Lavorato, J. F. Franco, M. J. Rider, and R. Romero, "Imposing radiality constraints in distribution system optimization problems," *IEEE Transactions on Power Systems*, vol. 27, no. 1, pp. 172–180, Feb. 2012.
[33] J. Liu, Z. Tang, P. P. Zeng, Y. L. Li, and Q. W. Wu, "Distributed adaptive expansion approach for transmission and distribution networks incorporating source-contingency-load uncertainties," *International Journal of Electrical Power & Energy Systems*, vol. 136, pp. 107711, Mar. 2022.
[34] J. Liu, Z. Tang, P. P. Zeng, Y. L. Li, and Q. W. Wu, "Fully distributed second-order cone programming model for expansion in transmission and distribution networks," *IEEE Systems Journal*, Mar. 2022.
[35] A. Shukla and S. N. Singh, "Multi-objective unit commitment using search space-based crazy particle swarm optimisation and normal boundary intersection technique," *IET Generation, Transmission & Distribution*, vol. 10, no. 5, pp. 1222–1231, Apr. 2016.
[36] H. Hosseinnia, J. Modarresi, and D. Nazarpour, "Optimal eco-emission scheduling of distribution network operator and distributed generator owner under employing demand response program," *Energy*, vol. 191, pp. 116553, Jan. 2020.
[37] J. L. Zhou, Y. N. Wu, C. H. Wu, Z. Q. Deng, C. B. Xu, and Y. Hu, "A hybrid fuzzy multi-criteria decision-making approach for performance analysis and evaluation of park-level integrated energy system," *Energy Conversion and Management*, vol. 201, pp. 112134, Dec. 2019.
[38] H. Rashidi and J. Khorshidi, "Exergoeconomic analysis and optimization of a solar based multigeneration system using multiobjective differential evolution algorithm," *Journal of Cleaner Production*, vol. 170, pp. 978–990, Jan. 2018.
[39] B. H. Qiao and J. Liu, "Multi-objective dynamic economic emission dispatch based on electric vehicles and wind power integrated system using differential evolution algorithm," *Renewable Energy*, vol. 154, pp. 316–336, Jul. 2020.
[40] A. D. Cioppa, C. De Stefano, and A. Marcelli, "Where are the niches? Dynamic fitness sharing," *IEEE Transactions on Evolutionary Computation*, vol. 11, no. 4, pp. 453–465, Aug. 2007.
[41] R. N. Allan, R. Billinton, I. Sjarief, L. Goel, and K. S. So, "A reliability test system for educational purposes-basic distribution system data and results," *IEEE Transactions on Power Systems*, vol. 6, no. 2, pp. 813–820, May 1991.
[42] J. S. Wang, F. Zhang, H. N. Liu, J. Y. Ding, and C. W. Gao, "Interruptible load scheduling model based on an improved chicken swarm optimization algorithm," *CSEE Journal of Power and Energy Systems*, vol. 7, no. 2, pp. 232–240, Mar. 2021.
[43] B. Hu, Y. Q. Tie, C. Z. Shao, M. Shahidehpour, T. Niu, C. Y. Li, and K. G. Xie, "A hierarchical transactive energy management framework for optimizing the reserve profile in district energy systems," *CSEE Journal of Power and Energy Systems*, vol. 7, no. 5, pp. 922–931, Sep. 2021.
[44] A. Wächter and L. T. Biegler, "On the implementation of an interior-point filter line-search algorithm for large-scale nonlinear programming," *Mathematical Programming*, vol. 106, no. 1, pp. 25–57, Mar. 2006.

**Jia Liu** received the B.S. and Ph.D. degrees in Electrical Engineering from Tianjin University, Tianjin, China, and Shanghai Jiao Tong University, Shanghai, China, in 2014 and 2019, respectively. He is currently a lecturer and postdoctor in Hangzhou Dianzi University, Hangzhou, China, and Zhejiang University, Hangzhou, China, respectively. He is the secretary-general of IEEE PES China Education Committee. His main research interests are planning, assessment and operation of power and energy systems, distributed optimization in transmission and distribution networks. Dr. Liu is an associate editor of Protection and Control of Modern Power Systems (PCMP).

**Pingliang Zeng** received the B.S. and Ph.D. degrees in Electrical Engineering from Huazhong University of Science and Technology, China, and Strathclyde University, U.K., in 1984 and 1990, respectively. He is currently a Professor in Hangzhou Dianzi University, Hangzhou, China. His current research interests are power system planning, integration of energy storage in low carbon electricity systems.

**Hao Xing** received the B.S. and Ph.D. degrees in Automatic Control from Zhejiang University, Hangzhou, China, in 2012 and 2017, respectively. He is an Associate Research Fellow of Department of Automation, Hangzhou Dianzi University, Hangzhou, China. His research interests are mainly distributed algorithms for control and optimization in smart grid.

**Yalou Li** received the B.S. degree in Electrical Engineering from Huazhong University of Science and Technology, Wuhan, China, in 1997. In 2000 and 2003, he received his M.S. and Ph.D. degrees respectively in Electrical Engineering from the China Electric Power Research Institute, Beijing, China, where he is currently a Chief Engineer. His main research interests are key devices digital simulation, analysis and control.

**Qiuwei Wu** obtained a Ph.D. degree in Power System Engineering from Nanyang Technological University, Singapore, in 2009. He has been working at the Department of Electrical Engineering, Technical University of Denmark (DTU) since Nov. 2009. His research interests are operations and control of power systems with high penetration of renewables, including wind power modeling and control, active distribution networks, and the operation of integrated energy systems.